Supplementary Information

# Effect of Ion Migration in Electro-Generated Chemiluminescence Depending on Luminophore Types and Operating Conditions

Sangbaie Shin,[a] Yunsung Park, [b] Sunghwan Cho,[c] Insang. You,[a] Inseok Kang, [b] Hong Chul Moon*[d] and Unyong Jeong*[a]

[a] Department of Materials Science and Engineering, Pohang University of Science and Technology, Cheongam-Ro 77, Nam-Gu, Pohang, Korea 790-784.

[b] Department of Chemical Engineering, Pohang University of Science and Technology, Cheongam-Ro 77, Nam-Gu, Pohang, Korea 790-784.

[c] Department of Materials Science Engineering, Yonsei University, 134 Shinchon-dong, Seoul, Korea.

[d] Department of Chemical Engineering, University of Seoul, Seoul 02504, Korea

*Corresponding author: ujeong@postech.ac.kr, hcmoon@uos.ac.kr

**Keywords:** Electro-generated chemiluminescence, Electromigration, Electrochemical reaction, Ion migration

# Guide of Supplementary Information

**Method :** Experimental details.

**Fig. S1:** Nyquist plots and CPE parameters for $Ir(diFppy)_2(bpy)PF_6$, DPA and $Ru(bpy)_3(PF_6)_2$ gels.

**Fig. S2:** Transient light emission profiles of $Ir(diFppy)_2(bpy)PF_6$ gel and DPA gel at various operating frequencies.

**Fig. S3:** Comparisons between the calculated light intensities and measured luminance of RGB gels.

**Fig. S4:** Comparisons of the transient current profiles at various operating frequencies and voltages of $Ru(bpy)_3Cl_2$ gel.

**Fig. S5:** Comparisons of the transient current profiles at various operating frequencies and voltages of $Ir(diFppy)_2(bpy)PF_6$ gel.

**Fig. S6:** Comparisons of the transient current profiles at various operating frequencies and voltages of DPA gel.

**Fig. S7:** Current profiles of ECL gel relative in different operating frequency conditions at same voltage (6Vpp).

**Fig. S8:** The results of solving mPNP equation.

**Fig. S9:** The concentration profile of luminophore density at the $5^{th}$ cycle of 50 Hz AC charging.

**Movie S1:** Operation movie of $Ru(bpy)_3Cl_2$ gel on a horizontally patterned electrode.

**Movie S2:** Operation movie of $Ir(diFppy)_2(bpy)PF_6$ gel on a horizontally patterned electrode.

**Movie S3:** Operation movie of DPA gel on a horizontally patterned electrode.

**Movie S4:** Operation movie of $Ru(bpy)_3(PF_6)_2$ on a horizontally patterned electrode.

**Table S1:** Evaluated parameters from Nyquist plot of $Ru(bpy)_3Cl_2$ gel as a function of various applied potentials.

**Table S2:** Evaluated parameters from Nyquist plot of $Ir(diFppy)_2(bpy)PF_6$ gel as a function of various applied potentials.

**Table S3.** Parameters extracted from Nyquist plot of DPA gel as a function of applied potential.

**Table S4.** Parameters extracted from Nyquist plot of $Ru(bpy)_3(PF_6)_2$ gel as a function of applied potential.

**Table S5.** Initial ion concentration inside electrolyte system and reaction constants.

## Methods

**Materials.** All materials except the green luminophore were purchased from Sigma-Aldrich: tris (2,2′-bipyridyl) dichlororuthenium (II) hexahydrate ($Ru(bpy)_3Cl_2$), iridium (III) chloride hydrate ($IrCl_3$), 2-(2,4-difluorophenyl)pyridine, ammonium hexafluorophosphate, 2-(2,4-difluorophenyl)pyridine, 2,2′-bipyridyl, 9,10-diphenylanthracene (DPA), 1-ethyl-3-methylimidazolium bis(trifluoromethylsulfonyl)imide (EMIM TFSI), tetrabutyl ammonium perchlorate (TBAP), polyvinyl acetate (PVAc, Mw = 500,000), polyvinyl pirrolidone (PVP, Mw = 380,000), polyethylene glycol (PEG, Mn = 10,000), and N-methyl-2-pyrrolidone (NMP). For green luminophore, 2,2′-bipyridylbis[2-(2′,4′-difluorophenyl)-pyridine] iridium(III) hexafluorophosphate ($Ir(diFppy)_2(bpy)PF_6$) was synthesized via a two-step reaction using a reflux system as described in the literature.[28] ITO/glass (sheet resistance 3−5 Ω/square, Asahi Glass Co., Ltd.) was used as a substrate. In order to clean the substrate surface, an ultrasonic precision cleaning process with acetone (5 min), isopropyl alcohol (IPA, 5 min), and de-ionized water (3 min) was performed sequentially. Polyimide tape and double-sided adhesive tape with thicknesses of 60 μm were used as spacers and insulators, respectively.

**Sample preparation and characterization.** To prepare the ECL gels, electrolytes and polymers were dissolved in advance. The concentration of the luminophores was varied from 3 to 5 wt% in the ECL gel. The formulations of the ECL gel were optimized for the luminophores to exhibit the best luminescence. 1-ethyl-3-methylimidazolium bis(trifluoromethylsulfonyl)imide) ([EMIM] [TFSI]) and tetrabutylammonium perchlorate (TBAP) were used as electrolytes. In particular, [EMIM] [TFSI] was employed for red emission gels, and TBAP in NMP was used for blue emissions. A mixture of [EMIM] [TFSI] and TBAP was used for green emissions. For a gel-formation host polymer, PVAc was used for all ECL gel. To improve the solubility of the luminophores, PEG and PVP were added to the green and blue ECL gel, respectively. The optimized weight ratios of the components in the ECL gel were as follows: [EMIM][TFSI]:PVAc = 10:0.5–3 for red, [EMIM][TFSI]:PVAc:PEG:TBAP = 10:0.5–3:1:1 for green, and NMP:PVAc:PVP:TBAP = 10:0.5–3:1:1 for blue. Each ECL gel was dot printed using a nozzle printer (IMAGE MASTER 350PC, Musashi. Eng. Inc.) on cleaned ITO/glass and Pt/Si substrate. The printing was used to obtain uniform device area of light emission. Then, the top electrode (ITO/glass) was covered, giving a simple sandwich configuration. A 60 μm-thick tape was used as a spacer to prevent

contacts between the top and bottom electrodes. All measurements were performed in ambient air. EIS measurements were performed using a potentiostat (SP-300, Bio Logic Inc.). To operate the ECL devices, AC voltage was applied using a waveform generator at high impedance mode (33220A, Agilent Tech. Inc.). For the measurements of optical properties, the luminance, emission spectrum, and CIE color coordinates were evaluated using a spectroradiometer (CS-2000, Konica Minolta Inc.) in a dark room. The transient optical properties and current profiles were evaluated using a silicon PIN photodiode (S6775, Hamamatsu Photonics) and 5Ω resistor within amplified using an pre-amplifier (SR570, Stanford research system). The amplified current was recorded on oscilloscope (S6775, Tektronix Co. Ltd.).

**Simulation conditions.**

Step 1. Solving modified Poisson-Nernst-Planck equations for DC condition. We used COMSOL Multiphysics software version 5.3 to solve the simulation. The coupled one-dimensional modified Poisson-Nernst-Boltzmann equations (mPNP) were solved. The solution for 10 ms was obtained with the time step of 0.1 ms. The equation is written as

$$\frac{\partial \square \square c_i}{\partial t} = D\nabla \cdot \left( c_i \left( 1 - N_A \sum_{i=1}^{n} a_i^3 c_i \right) \nabla \frac{z_i e \phi}{k_B T} + \left( 1 - N_A \sum_{i=1}^{n} a_i^3 c_i \right) \nabla c_i + N_A a_i^3 c_i \sum_{i=1}^{n} \nabla c_i \right) \quad (1)$$

$$-\varepsilon \varepsilon_0 \nabla \cdot (\nabla \phi) = \rho = F \sum_{i=1}^{n} z_i c_i \quad (2)$$

$N_A$ : The Avogadro number, $c_i$ : The ion concentration [M] of species i

$a_i$ : The ion size of ion species i, $z_i$ : Valence number of species i

e : The elementary charge, $k_B$ : Boltzmann constant,

$\phi$ : The electric potential, F : Faraday constant,

D : Diffusion coefficient, $10^{-10}$ $m^2/s$, T : The temperature, 300 K

The total length of simulation system was 100 μm. The electrode potential at the left end was set to 0 and 3 V at the right end with zero flux of ion from ion gel boundary. We made the redox reaction exclusively take place only when the electric field was higher than 3 V/100 μm

near both electrodes, to take place within EDL. The redox reaction is considered to be a first order reaciton, $k_1[Ru(bpy)_3^{2+}]$. We calculated the redox reaction constant $k_1$ empirically by considering 30% conversion in 1.0 μs in the first order reaction to obtained 2.23 * $10^5$ $s^{-1}$. The left electrode was set as cathode and $Ru(bpy)_3^{+}$ ion formed while consuming $Ru(bpy)_3^{2+}$ ion at the same rate. The right electrode was set as anode and $Ru(bpy)_3^{3+}$ is formed. The initial weight fraction of $Ru(bpy)_3Cl_2$ was 5.0 wt% in the EMIM-TFSI electrolyte, which corresponds to 3.12 mol% of $Ru(bpy)_3^{2+}$ in the total cations. Considering the molecular volume of the EMIM-TFSI, the size of the ions was fixed to be 0.55 nm and the maximum ion concentration (9.981 M) was calculated based on the size of the ions. The initial concentrations of ions, the maximum concentration that the all ions can reach, and reaction constants are shown in Table S5. The constructed mesh was non-uniform. The mesh in region within 2 nm from both electrodes had 800 uniform elements with size of 5 * $10^{-12}$ m. The other region had 15000 non-uniform mesh elements with size of 6.66 * $10^{-9}$ m in average, with smaller mesh near electrode.

Step 2. Solving the Nernst-Planck equation (Eq. 1) for AC condition with fitted electric field from mPNP eqautions. The initial ion concentration, maximum ion concentration, and redox reaction constant was same as in Step 1. We made the redox reaction exclusively take place in region within 1 nm from both electrodes, which was estimated length of EDL. The recombination reaction was $2^{nd}$ order reaction with reaction rate represented as $k_2[Ru(bpy)_3^{1+}][Ru(bpy)_3^{3+}]$. The reaction constant of $k_2$ was $10^{10}$ $M^{-1}s^{-1}$, which was obtained from a reported annihilation reaction constant of $Ru(bpy)_3^{2+}$. We solved the equation in Step 2. with DC and AC condition. We solved for 5 cycles of 5 Hz and 50 Hz condition as AC condition, which is 1 s and 0.1 s, respectively. The time step was set as one fourth of each period, respectively. The direction of electric field and the anode and cathode were reversed every half of the period. The mesh in region within 1 nm from both electrodes had 200 uniform elements with the size of $10^{-11}$ m. The other region had 5000 non-uniform mesh elements with size of 2.00 * $10^{-9}$ m in average, with smaller mesh near electrodes.

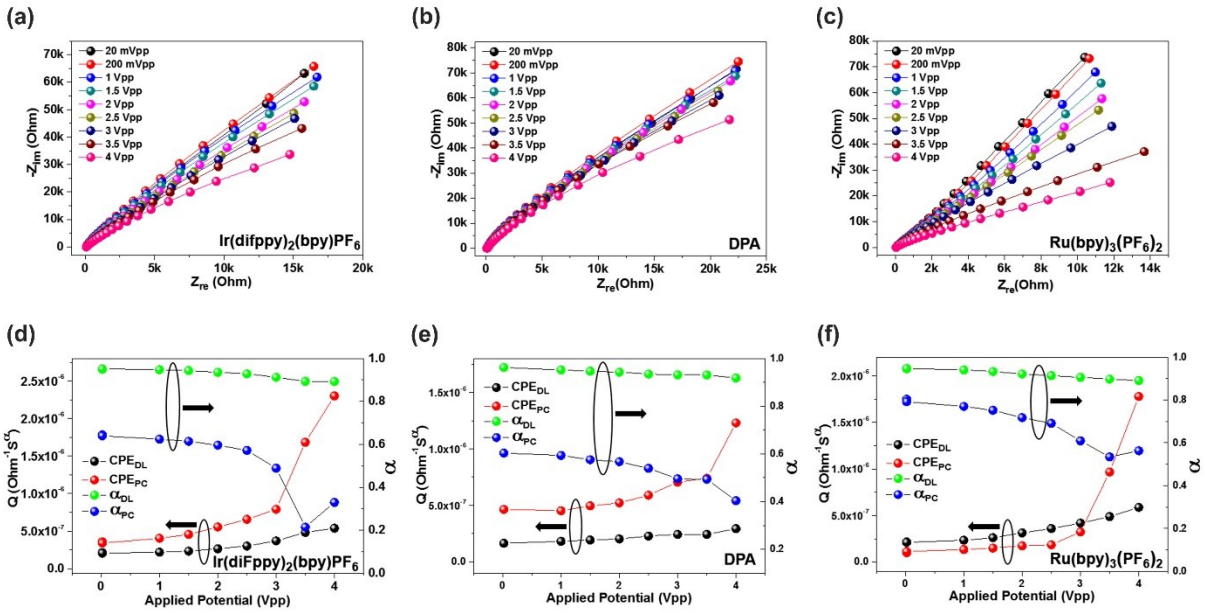


**Fig. S1.** Nyquist plots and CPE parameters for $Ir(diFppy)_2(bpy)PF_6$, DPA, and $Ru(bpy)_3(PF_6)_2$ gels. (a–c) Nyquist plots of $Ir(diFppy)_2(bpy)PF_6$, DPA, and $Ru(bpy)_3(PF_6)_2$ gels as a function of applied voltage. (d–f) Extracted CPE parameters as a function of applied voltage. Electrochemical impedance measurements were performed using a cell with 1 mm in diameter and 60-μm in thickness. The impedance was recorded at the frequency range of 1 MHz to 10 Hz. Subsequent measurements were conducted after at least 5 min to reduce the influence of previous measurements. The CPE parameters were evaluated by fitting the experimental data to the equivalent circuit model.

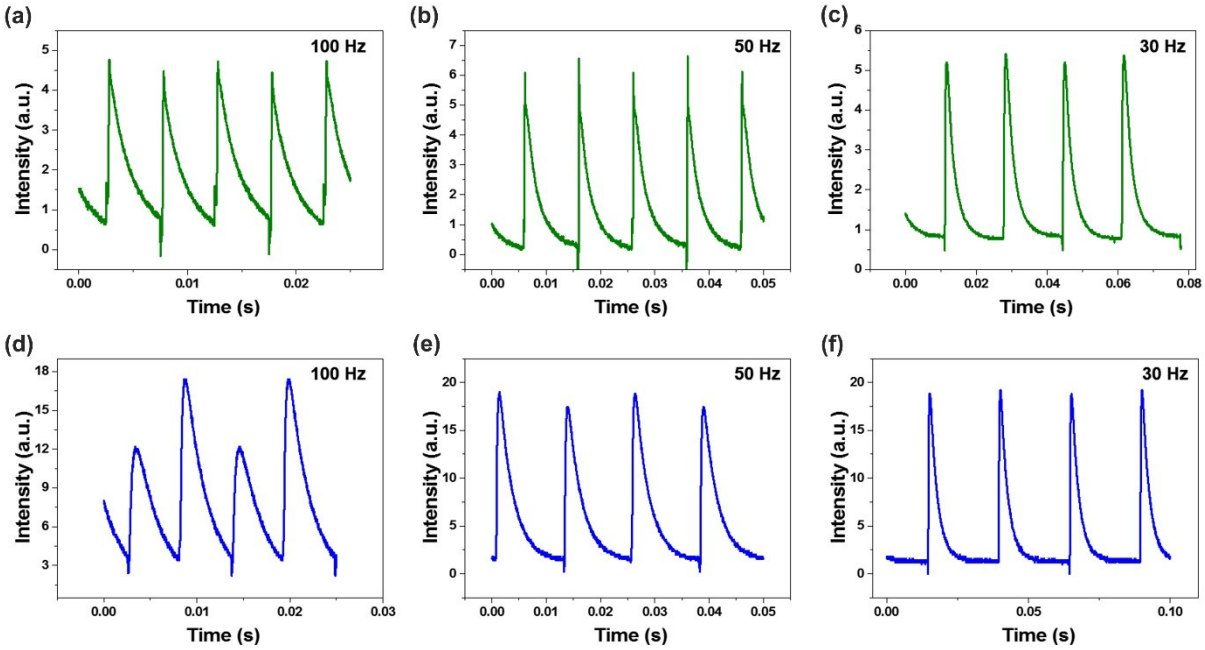


**Fig. S2.** Transient light emission profiles of $Ir(diFppy)_2(bpy)PF_6$ gel and DPA gel at various operating frequencies. Emission profiles of (a–c) $Ir(diFppy)_2(bpy)PF_6$ gel and (d–f) DPA gel. Devices were prepared with a diameter of 3 mm and a 60-µm-thick spacer between two identical ITO electrodes. The operating voltages were 5.6 and 6.5 $V_{pp}$ for $Ir(diFppy)_2(bpy)PF_6$ and DPA gels, respectively. The emission profiles were recorded on a photodiode with a pre-amplifier.

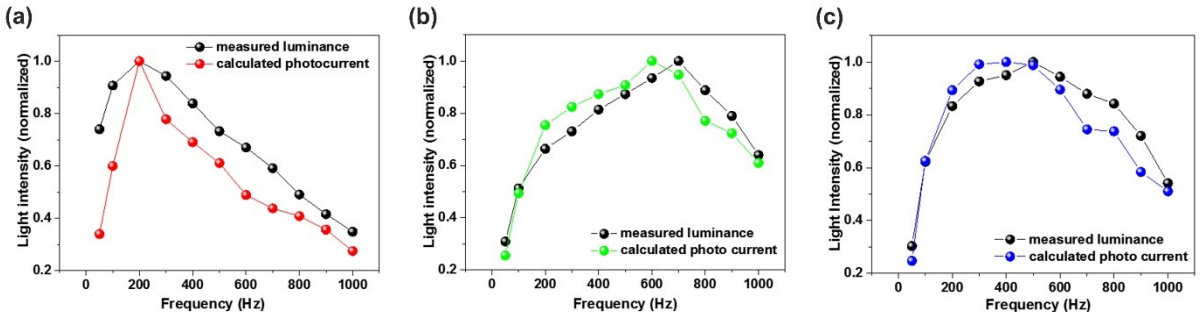


**Fig. S3.** Comparisons between the calculated light intensities and measured luminance of $Ru(bpy)_3Cl_2$ gel, $Ir(diFppy)_2(bpy)PF_6$ gel, and DPA gel. Each integrated light intensity was multiplied by corresponding frequency to obtain the emission intensity during the same period. (a) $Ru(bpy)_3Cl_2$ gel. (b) $Ir(diFppy)_2(bpy)PF_6$ gel. (c) DPA gel.

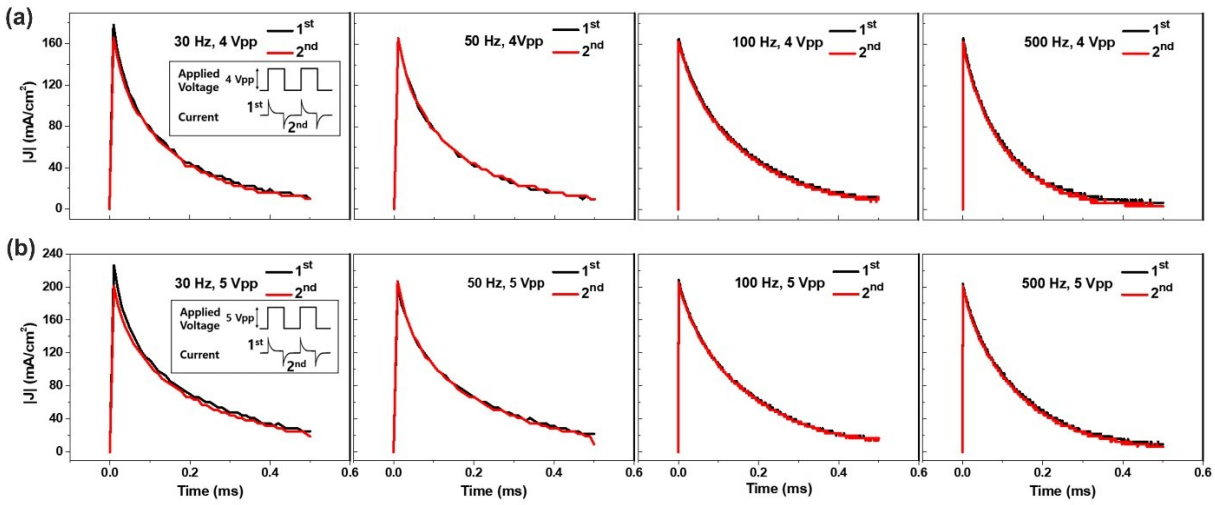


**Fig. S4.** Comparisons of the transient current profiles at various operating frequencies and voltages (30, 50, 100, 500 Hz and 4, 5 $V_{pp}$) of the $Ru(bpy)_3Cl_2$ gel. The insets in the left column represent the operation cycles. The 1st and 2nd current profiles are the operation cycle of red emitting gel. The 2nd profiles were inverted to compare with the 1st profiles.

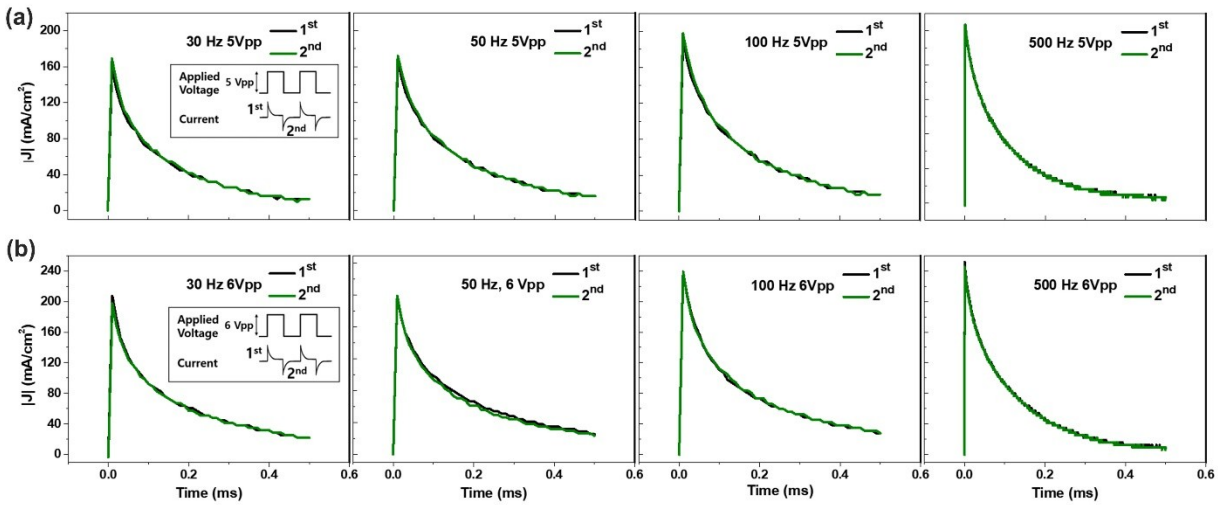


**Fig. S5.** Comparisons of the transient current profiles at various operating frequencies and voltages (30, 50, 100, 500 Hz and 5, 6 $V_{pp}$) of the $Ir(diFppy)_2(bpy)PF_6$ gel. The insets in the left column represent the operation cycles. The 1st and 2nd current profiles are the operation cycle of green emitting gel. The 2nd profiles were inverted to compare with the 1st profiles.

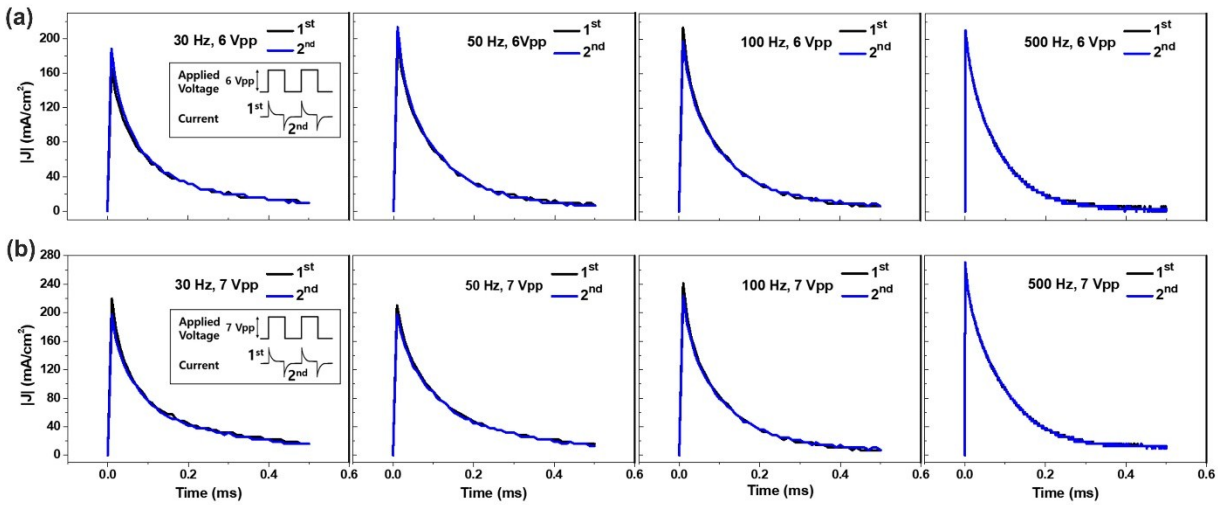


**Fig. S6.** Comparisons of the transient current profiles at various operating frequencies and voltages (30, 50, 100, 500 Hz and 5, 6 $V_{pp}$) of the DPA gel. The insets in the left column represent the operation cycles. The 1st and 2nd current profiles are the operation cycle of blue emitting gel. The 2nd profiles were inverted to compare with the 1st profiles.

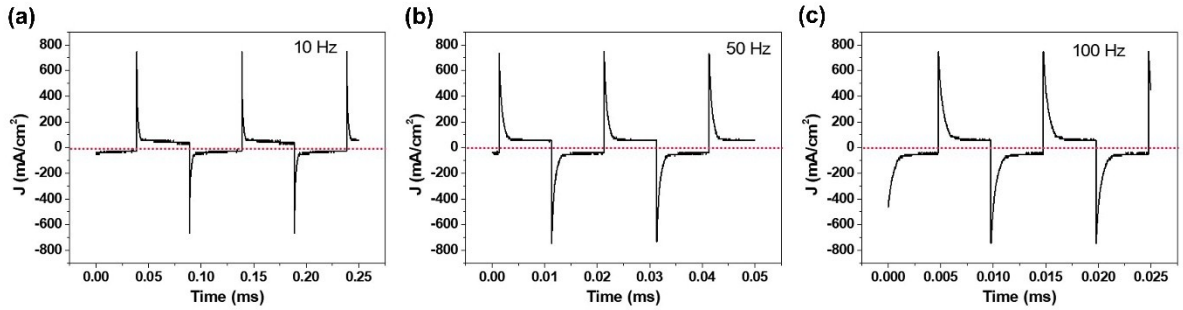


**Fig. S7.** Current profiles of ECL gel relative in different operating frequency conditions at same voltage (6 Vpp). (a) 10 Hz. (b) 50 Hz. (c) 100 Hz.

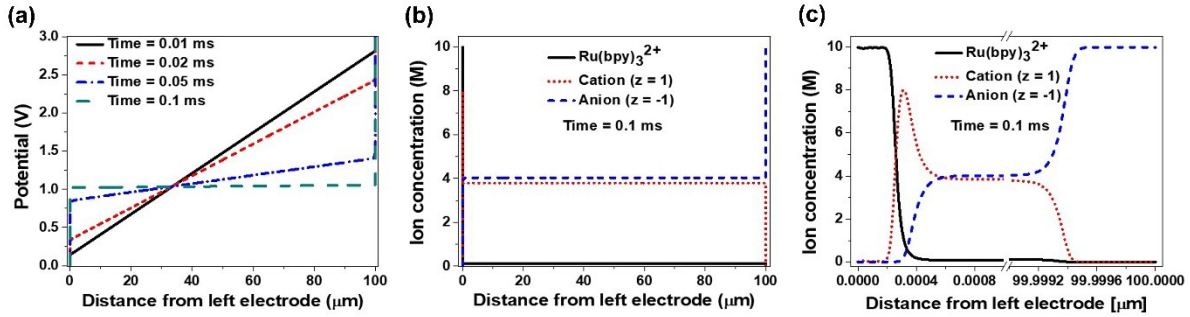


**Fig. S8.** The results of solving mPNP equation, 3 V is applied across the ion gel of 100 μm without reaction. (a) The electric potential distribution across the ion gel at time 0.01 ms, 0.02 ms 0.05 ms, and 0.1 ms. (b) The ion concentration distribution at time 0.1 ms (c) The ion concentration distribution near EDL at time 0.1 ms.

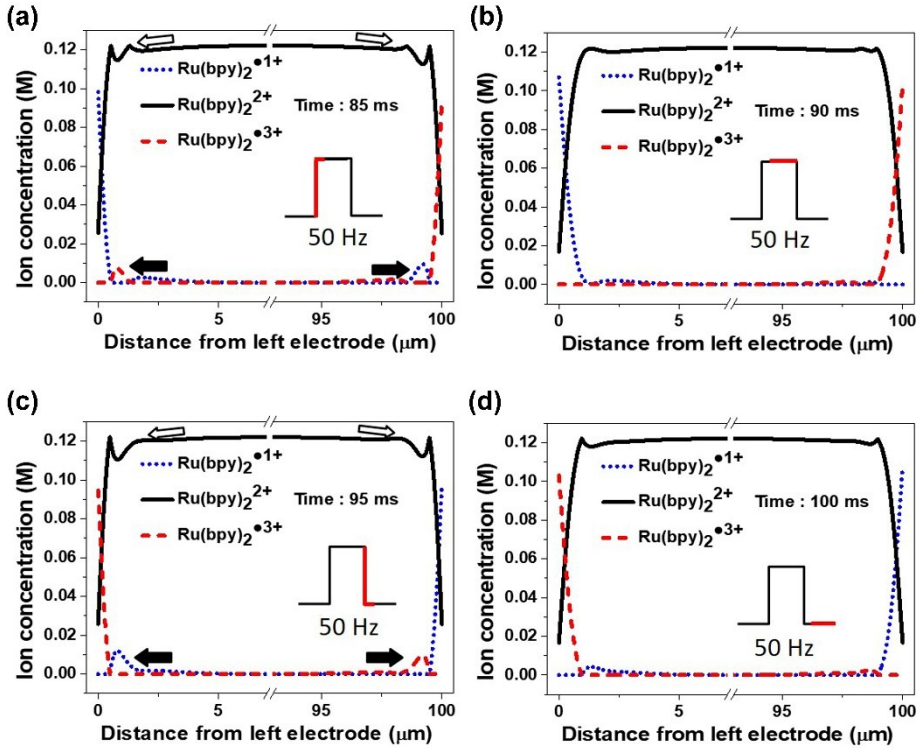


**Fig. S9.** The concentration profile of luminophore density at the 5th cycle of 50 Hz AC charging. (a) concentration profile at 85 ms. (b) concentration profile at 90 ms. (c) concentration profile at 95 ms. (d) concentration profile at 100 ms.

**Table S1.** Parameters extracted from Nyquist plot of $Ru(bpy)_3Cl_2$ gel as a function of applied potential.

| Potential | $R_s(\Omega)$ | $CPE_{(DL)}$ $Q/(\Omega^{-1}s^{\alpha})$ | $\alpha_{dl}$ | $R_{ct}(\Omega)$ | $CPE_{(PC)}$ $Q/(\Omega^{-1}s^{\alpha})$ | $\alpha_{pc}$ | $\chi^2$ |
|---|---|---|---|---|---|---|---|
| 20mVpp | 47.79 | 3.255E-07 | 0.9513 | 7268 | 6.659E-07 | 0.6687 | 0.001691 |
| 200mVpp | 48.81 | 3.105E-07 | 0.9542 | 6847 | 6.322E-07 | 0.6654 | 0.00056 |
| 1Vpp | 48.95 | 3.215E-07 | 0.9514 | 6428 | 6.402E-07 | 0.6604 | 0.003632 |
| 1.5Vpp | 49.25 | 3.324E-07 | 0.9493 | 5737 | 6.594E-07 | 0.6558 | 0.001095 |
| 2Vpp | 49.02 | 3.651E-07 | 0.943 | 5649 | 7.108E-07 | 0.6417 | 0.002389 |
| 2.5Vpp | 48.77 | 3.925E-07 | 0.9381 | 5538 | 7.437E-07 | 0.628 | 0.004614 |
| 3Vpp | 48.65 | 4.627E-07 | 0.9272 | 1704 | 1.272E-06 | 0.55 | 0.01852 |
| 3.5Vpp | 48.61 | 4.326E-07 | 0.9334 | 332.9 | 2.655E-06 | 0.5492 | 0.003057 |
| 4Vpp | 48.15 | 5.501E-07 | 0.9084 | 19.81 | 3.129E-06 | 0.4893 | 0.07006 |

**Table S2.** Parameters extracted from Nyquist plot of $Ir(diFppy)_2(bpy)PF_6$ gel as a function of applied potential.

| Potential | $R_s(\Omega)$ | $CPE_{(DL)}$ $Q/(\Omega^{-1}S^{\alpha})$ | $\alpha_{dl}$ | $R_{ct}(\Omega)$ | $CPE_{(PC)}$ $Q/(\Omega^{-1}S^{\alpha})$ | $\alpha_{pc}$ | $\chi^2$ |
|---|---|---|---|---|---|---|---|
| 20mVpp | 50.11 | 2.161E-07 | 0.9453 | 22799 | 1.004E-07 | 0.8034 | 0.00769 |
| 200mVpp | 49.98 | 2.113E-07 | 0.9473 | 25817 | 1.141E-07 | 0.792 | 0.005526 |
| 1Vpp | 50.62 | 2.339E-07 | 0.9403 | 26783 | 1.342E-07 | 0.7702 | 0.006917 |
| 1.5Vpp | 50.87 | 2.614E-07 | 0.933 | 30174 | 1.507E-07 | 0.7521 | 0.001266 |
| 2Vpp | 50.33 | 3.135E-07 | 0.9215 | 32885 | 1.742E-07 | 0.7174 | 0.005998 |
| 2.5Vpp | 50.13 | 3.599E-07 | 0.9135 | 44716 | 1.849E-07 | 0.6911 | 0.0112 |
| 3Vpp | 49.97 | 4.182E-07 | 0.9057 | 56800 | 3.239E-07 | 0.6095 | 0.01732 |
| 3.5Vpp | 49.26 | 4.882E-07 | 0.8976 | 38167 | 9.673E-07 | 0.5342 | 0.03125 |
| 4Vpp | 48.74 | 5.867E-07 | 0.8908 | 17142 | 1.778E-06 | 0.5629 | 0.06364 |

**Table S3.** Parameters extracted from Nyquist plot of DPA gel as a function of applied potential.

| Potential (V) | $R_s(\Omega)$ | $CPE_{(DL)}$ $Q/(\Omega^{-1}S^{\alpha})$ | $\alpha_{dl}$ | $R_{ct}(\Omega)$ | $CPE_{(PC)}$ $Q/(\Omega^{-1}S^{\alpha})$ | $\alpha_{pc}$ | $\chi^2$ |
|---|---|---|---|---|---|---|---|
| 20mVpp | 72.77 | 2.131E-07 | 0.9498 | 20617 | 3.576E-07 | 0.6447 | 0.000733 |
| 200mVpp | 75.81 | 2.072E-07 | 0.9515 | 20741 | 3.408E-07 | 0.6396 | 0.000599 |
| 1Vpp | 76.63 | 2.183E-07 | 0.948 | 16818 | 4.044E-07 | 0.6243 | 0.000858 |
| 1.5Vpp | 76.7 | 2.34E-07 | 0.9434 | 13738 | 4.554E-07 | 0.6143 | 0.001976 |
| 2Vpp | 76.49 | 2.65E-07 | 0.936 | 8768 | 5.558E-07 | 0.5961 | 0.006034 |
| 2.5Vpp | 76.27 | 3.013E-07 | 0.9283 | 3398 | 6.571E-07 | 0.5721 | 0.00156 |
| 3Vpp | 74.92 | 3.699E-07 | 0.9129 | 1897 | 7.912E-07 | 0.4891 | 0.0283 |
| 3.5Vpp | 73.98 | 4.829E-07 | 0.8935 | 604.33 | 1.683E-06 | 0.2145 | 0.03948 |
| 4Vpp | 73.88 | 5.382E-07 | 0.8928 | 20.03 | 2.301E-06 | 0.3298 | 0.06381 |

**Table S4.** Parameters extracted from Nyquist plot of $Ru(bpy)_3(PF_6)_2$ gel as a function of applied potential.

| Potential (V) | $R_s(\Omega)$ | $CPE_{(DL)}$ $Q/(\Omega^{-1}S^{\alpha})$ | $\alpha_{dl}$ | $R_{ct}(\Omega)$ | $CPE_{(PC)}$ $Q/(\Omega^{-1}S^{\alpha})$ | $\alpha_{pc}$ | $\chi^2$ |
|---|---|---|---|---|---|---|---|
| 20mVpp | 108.8 | 1.641E-07 | 0.9624 | 27501 | 4.649E-07 | 0.6034 | 0.003673 |
| 200mVpp | 111.3 | 1.698E-07 | 0.9579 | 35312 | 4.206E-07 | 0.6003 | 0.00377 |
| 1Vpp | 111.4 | 1.816E-07 | 0.9519 | 33987 | 4.525E-07 | 0.5938 | 0.004522 |
| 1.5Vpp | 111.9 | 1.934E-07 | 0.9468 | 30586 | 4.957E-07 | 0.5756 | 0.006005 |
| 2Vpp | 112.3 | 2.028E-07 | 0.9427 | 26253 | 5.221E-07 | 0.5672 | 0.007956 |
| 2.5Vpp | 112.7 | 2.286E-07 | 0.9348 | 24875 | 5.9E-07 | 0.5395 | 0.01045 |
| 3Vpp | 113.3 | 2.429E-07 | 0.9316 | 17239 | 7.059E-07 | 0.4957 | 0.01297 |
| 3.5Vpp | 113.6 | 2.431E-07 | 0.931 | 2304 | 7.413E-07 | 0.4935 | 0.01884 |
| 4Vpp | 115.6 | 2.932E-07 | 0.9184 | 840.4 | 1.23E-06 | 0.4035 | 0.02373 |

**Table S5.** Initial ion concentration inside electrolyte system and reaction constants

| Properties | Value |
|---|---|
| Maximum concentration | 9.981 M |
| Initial $Ru(bpy)_3^{+}$ | 0 |
| Initial $Ru(bpy)_3^{2+}$ | 0.122 M |
| Initial $Ru(bpy)_3^{3+}$ | 0 |
| Non-reactive cation (valence : 1) | 3.788 M |
| Non-reactive anion (valence : -1) | 4.032 M |
| Redox reaction constant $k_1$ | $2.23 * 10^5$ $s^{-1}$ |
| Recombination reaction constant $k_2$ | $10^{10}$ $M^{-1}s^{-1}$ |